UNIVERSITAT DE BARCELONA

A study of the shortwave schemes in the Weather Research and Forecasting model

Alex Montornès Torrecillas

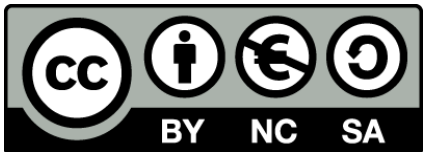

Chapter 7

Conclusions

The main objective of this thesis was the identification and evaluation of the sources of error that contribute directly or indirectly to the skills of the solar schemes used by NWP models and, particularly, in the WRF-ARW model. Nevertheless, the development of the research presented in the previous chapters showed a lack in the documentation of the shortwave parameterizations from the theoretical point of view as well as from the coding perspective. In order to address this issue, a secondary objective was added by including a scientific report which summarizes and discusses all the approaches included in the solar schemes available in the WRF-ARW model, presented in Chapter 3.

The discussion of the elements that determine the skills of the shortwave schemes led to identify two kind of contributions (Eq. 4.3): i) sources of error and ii) sources of uncertainty. On the one hand, the sources of error were defined such as all these elements intrinsic to the solar parameterization. In other words, the simplification of the RTE and the parameterization of the radiative variables as a function of the meteorological variables of the model. On the other hand, the sources of uncertainty were related with all the external factors to the shortwave scheme that can contribute to the accuracy of the irradiances (e.g. other physical schemes, coarse model predictability).

The sources of error were divided into three contributions: ϵ_{tom} due to the definition of a TOM lower than the real TOA, ϵ_{trun} as a consequence of the vertical discretization of the atmosphere in a set of few layers assumed as homogeneous and ϵ_{phys} due to the physical assumptions in the radiative transfer problem.

In order to neglect the contribution of the sources of uncertainty, the method used for the study of ϵ_{tom}, ϵ_{trun} and ϵ_{phys} consisted in the preparation of a sandbox tool in which six solar schemes were tested: Dudhia, Goddard, New Goddard, CAM, RRTMG and FLG. In this sandbox tool, the code of the solar schemes was prepared for working with 1-dimensional vertical profiles by using identical atmospheric conditions for all the schemes. By means of this tool, multiple experiments were performed, presenting a full discussion of ϵ_{tom} and ϵ_{trun} in Chapter 5 and of ϵ_{phys} under clear sky cases in Chapter 6.

A consistent set of input conditions was used for all the shortwave parameterizations to enable a rigorous comparison of how each scheme represented the main physical processes (e.g. water vapor absorption, the Rayleigh scattering, the shortwave heating rate), as it was discussed in Sect. 5.3 and 6.3.

The discussion presented in Chapter 3 as well as the results exposed in Chapters 5 and 6 lead to a natural division of the conclusions of this thesis in two blocks: i) physical processes and ii) sources of error.

Physical processes

The set of experiments presented in Sects. 5.3 and 6.3 by using the same input vertical profiles address a full comparison of the physical processes modeled by each parameterization. This comparison can be related to formulation details of each of the shortwave schemes that are presented in Chapter 3. The conclusions derived from these results will be detailed in the following points and summarized in the infograph presented in Fig. 7.1.

- **Dry gaseous attenuation/absorption**:

  Solar schemes represent the attenuation of the solar beam due to the dry atmospheric gases by assuming a small set of species that are significantly active in the shortwave range of the electromagnetic spectrum. As these species are not individually represented by the Euler equations, solar parameterizations consider fixed concentration values that vary from one scheme to the other. Ozone and carbon dioxide are two relevant species due to their importance in the radiative transfer computation in the UV and near-IR regions, respectively.

  In the case of ozone, the important latitudinal, vertical and temporal variations of this species provides incentive for the shortwave parameterizations to employ some type of representation of these variations. The schemes use fixed ozone profiles for this purpose with varying amount of detail. The RRTMG has the simplest representation and the CAM scheme has the greatest detail. The ozone profile specifications as well as an evaluation of the error introduced by this simplification were discussed in Montornès et al. (2015d). The results indicated that the maximum deviations were over the poles and showed prominent longitudinal patterns due to the lack of representation of the patterns associated with the Brewer–Dobson circulation and the quasi–stationary features forced by the land-sea distribution. These simplifications introduce spatial and temporal biases with near-zero departures over the tropics throughout the year and increasing poleward with a maximum in the high middle latitudes during the winter of each hemisphere.

  CO_2 shows a wide range of values throughout the solar schemes, from the lowest concentration in Goddard, with 300 ppmv, to the highest value in RRTMG, with 376 ppmv. CAM has the highest temporal detail with a database from 1869 to 2101, based on the A2 scenario used in the IPCC report (Sankovski et al., 2000).

  The effect of each specie is included by different spectral bands that, generally, are not overlapped. At each band, the gas amount is evaluated as a function of the total dry air and, finally, the optical thickness is determined by using internal absorption coefficients determined from spectral data-sets such as the HITRAN.

  Dudhia is a particular case in which the effect of the dry atmosphere is represented as a function of a parameter called swrad_scat and the total dry air mass in a broadband integration approach.

  As a consequence of the distinct approaches in the treatment of the atmospheric gases, shortwave schemes model different degrees of opacity. The RRTMG is the parameterization with the highest attenuation for three reasons: i) it is the scheme with the larger number of atmospheric species (O_3, CO_2, O_2, CH_4), ii) it assumes the highest CO_2 concentration and iii) it considers a broad range of the thermal-IR region as a part of the solar range, producing an increment of the absorption by carbon dioxide.

  Goddard and New Goddard are intermediate cases with significant differences although they are based on the same technical reports, being Goddard more transparent than New Goddard. These differences are a consequence of two improvements in New Goddard: i) an increment of the CO_2 concentration and ii) an increment of the k_{O_3} coefficient in the PAR region.

FLG shows a similar attenuation than Goddard. It is important to consider that this scheme may deal with minor gases such as CO_2, O_2, CH_4, N_2O, among others, but they are disabled in the default version of the code via the variable called NGAS, leading to a more transparent atmosphere.

Finally, CAM and Dudhia are the parameterizations with the lower attenuation of the direct beam. The case of CAM is explained because the O_3 and CO_2 absorbs radiation in narrow bands, decreasing the total effect in the whole spectrum. Moreover, the dependence of the CO_2 with the year, based on the A2 scenario of the IPCC report, could vary the results obtained in the experiments presented in this thesis.

Furthermore, the attenuation produced by Dudhia is directly dependent on the parameter swrad_scat, but, in its default version, this scheme becomes the most transparent one.

- **Water vapor absorption**: The absorption due to water vapor is included following two approaches. Some schemes, such as Dudhia, use empirical relationships while the most complex parameterizations, such as the RRTMG, include the CKD method in order to consider the high variation of the absorption coefficient with the wavelength. Other schemes use pseudo CKD methods or directly the gray atmosphere approach in some spectral intervals.

  As water vapor is a solution of the dynamics of the model, the resolved profile is directly used in the radiative transfer computation. Therefore, the differences between solar schemes are produced basically by three factors: i) the range of the solar spectrum considered, ii) the method applied and iii) the data-sets used for the absorption coefficient.

  The scheme that represents the highest absorption level is CAM. This scheme is followed by RRTMG, New Goddard, FLG and Dudhia, being Goddard the most transparent one.

  The significant differences between Goddard and New Goddard are a consequence of the effect of the water vapor in the PAR region of the spectrum (Table 3.4) and hence, increasing the amount of absorbed energy with respect to the old version.

- **Cloud ice crystals attenuation**: The complex relationship between the solar radiation and the ice crystals is simplified by defining an effective radius of the particles that generally depends on the temperature and the IWC. Some schemes include more sophisticated approaches by adding other variables such as the land/ocean flag or even the latitude region.

  With this variable, the optical thickness is expressed as a function of the IWC and a polynomial in terms of the inverse of $r_{e,i}$. The coefficients of this polynomial fit empirical data-sets. Therefore, the differences in the beam attenuation between the parameterizations are mostly related on the determination of $r_{e,i}$ and the aforementioned coefficients.

  The RRTMG is the scheme that shows the highest attenuation of the solar beam when ice crystals are present. The New Goddard, CAM and FLG schemes produce much lower attenuation values.

  Dudhia is the parameterization that represents the least attenuation due to the ice crystals. Apart of the wide simplifications assumed by this scheme, the main element that contribute to this transparency is the evaluation of the variable called effective water liquid mixing ratio defined in Eq. 3.14. In this equation, the contribution of the q_i is reduced to the 10% with respect to the original value, reducing the impact of this hydrometeor.

Figure 7.1: Infograph summarizing the relative magnitude of the physical processes calculated by each solar parameterization using identical input data. The '+'/'-' scale indicates the relative magnitude with schemes closer to the '+' producing larger magnitudes for the designated parameter. A gray letter for a scheme indicates that no calculation is available for that parameter from that scheme. The information presented in this figure is derived from Sects. 5.3, 6.3 and Montornès et al. (2015e).

The representation of ice crystals in Goddard could not be analyzed in the experiments presented in this thesis. Due to the large threshold for detecting clouds, this scheme modeled a clear-sky atmosphere in all the cases.

- **Cloud water droplets attenuation**: The complex problem of the cloud droplets is solved with an approach that is similar to the one used for ice crystals. With the exception of Dudhia, solar schemes define an effective radius, $r_{e,l}$, using simpler approaches than in the previous case. Then, the optical thickness is determined as a function of the LWC and a polynomial expressed in terms of $r_{e,l}^{-1}$.

  In the experiments presented in this thesis, all the parameterizations, with the exception of Dudhia, produce similar attenuation behaviors. All of them attenuate the solar beam completely, leading to zero DHI values. The main differences between schemes arise from the rate of attenuation inside the cloud, presented in Fig. 5.10. The RRTMG and FLG are the schemes that attenuate the direct beam faster, while Goddard, New Goddard and CAM show a slightly slower reduction inside the cloud.

  In contrast, Dudhia represents a more transparent cloud avoiding a zero value in the GHI, necessary because this scheme does not solve the DIF explicitly.

- **Rayleigh scattering**: The effects of the molecular scattering are not evaluated explicitly for each gaseous specie. Instead of this, the Rayleigh scattering is determined at each band assuming directly the dry air mass and an extinction coefficient determined from data-sets such as the HITRAN. The single scattering albedo and the asymmetry factor are set as 1. Therefore, the elements that determine the differences between shortwave schemes are the aforesaid extinction coefficient and the method used for the approximation of the source function in the solution of the RTE.

  FLG and New Goddard model a similar Rayleigh scattering contribution while CAM produces the least diffuse atmosphere. RRTMG and Goddard show an intermediate scattering degree.

  The differences between Goddard and New Goddard are a consequence that the newest scheme includes the Rayleigh scattering in two bands of the near-IR region which are not considered in the previous one (Table 3.4).

- **Mie scattering by cloud ice crystals**: Following the same approach that in the case of the beam attenuation, the scattering variables for the ice crystals are determined as a function of one polynomial in terms of $r_{e,i}$.

  Therefore, given one cloud, the degree of scattering just depends on the set approximations for determining $r_{e,i}$, the coefficients of the polynomials and the method used for approximating the source function in the RTE, necessary for the evaluation of the diffuse component.

  The RRTMG is the scheme that produces the highest scattering. New Goddard, FLG and CAM produces similar values because it is the parameterization that generates the lowest diffuse values.

- **Mie scattering by cloud water droplets**: The scattering due to the water droplets is parameterized with a method similar the one employed for ice crystals.

  CAM and Goddard are the schemes that model the most scattering droplets, followed by New Goddard and RRTMG. Finally, FLG is the parameterization that produces the lowest scattering.

- **Solar heating by dry gases**: The analysis of the heating rate by the different parameterizations reveals similar values for all the schemes with the exception of Dudhia and

RRTMG. On the one hand, the attenuation of the direct beam in Dudhia does not contribute in the heating rate as it is shown in Eq. 3.8 and hence, the absorption is zero in this parameterization. On the other hand, the RRTMG produces a higher heating rate with respect to the other schemes due to the effect of the large number of active species.

- **Solar heating by water vapor**: The experiments conducted as part of this thesis indicate that the FLG parameterization yields a much higher water vapor absorption than all of the other schemes. CAM, Goddard and New Goddard show intermediate absorption similar one to each other. Finally, the RRTMG is the scheme that produces the lower warming due to the water vapor. The approximation used by Dudhia produces a realistic heating rate although it is slightly lower than in the other schemes. These results are in the line of the ones observed in Montornès et al. (2015e) using real simulations.

- **Solar heating by stratospheric ozone**: FLG is the scheme that shows the highest heating rate in the stratosphere due to the ozone profile while New Goddard and Goddard are the schemes that produce the lowest absorption. The fact that these three schemes use the same ozone profiles and similar spectral ranges for this gas but they produce different behaviors indicates that the coefficients used for evaluating the optical thickness play an important role. The RRTMG and CAM perform intermediate heating rates.

  The presence of an ozone profile in the stratosphere is essential for real simulations with an horizon longer than one day, as we discussed in Montornès et al. (2015e). This paper showed that in the first 24 h of the simulation, the thermal structure of the stratosphere is mainly driven by the information of the coarse model, while, for longer simulation horizons, the ozone profiles become a critical issue. In the case of Dudhia, without any O_3, the thermal inversion of the stratosphere breaks down progressively.

- **Solar heating by ice clouds**: Dudhia is the scheme that produces the highest heating rate inside an ice cloud. Regarding the schemes that solve the RTE explicitly, FLG is the scheme that absorbs more energy inside the cloud, RRTMG and New Goddard produce an intermediate absorption level and CAM is the parameterization with the lowest heating rate. This behavior is the opposite to the beam attenuation and the scattering ones, indicating the high efficiency of the source function transforming the direct beam in scattered light.

- **Solar heating by water clouds**: The behavior inside water clouds is exactly the opposite than for ice clouds. The schemes with a larger attenuation of the direct beam produce the highest heating rates and the lowest scattering. Hence, FLG is the scheme that absorbs the highest amount of radiation, followed by New Goddard, Goddard (both with similar values) and RRTMG. Finally, CAM is the parameterization with the lower heating rate inside the cloud.

- **Importance of the RTE solution and the parameterization of the radiative variables**: The fact that schemes using the same solution of the RTE experience different degrees of attenuation and scattering indicates that the parameterization of the radiative variables play a more relevant role.

- **Role of the shortwave schemes in NWP models**: The set of studies presented in Montornès et al. (2015e) and Montornès et al. (2016c) show that the relationship between the solar parameterizations and the other elements of the model goes beyond the simple representation of the day/night patterns. The output of the solar schemes interacts with the other parts of the NWP model through the LSM scheme and the diabatic term of the energy equation. Consequently, the differences in the evaluation of the shortwave heating rate and the surface fluxes lead to different results in the other meteorological variables, that increase with the simulation horizon.

Sources of error

The evaluation of the sources of error presented in Sects. 5.3 and 6.3 lead to the following conclusions, summarized in the infographs presented in Figs. 7.2 and 7.3.

- **Top of the Model (TOM) error** (Fig. 7.2): The set of studies presented in this thesis reveal that the impact of the TOM error is significantly low. For the typical TOM values used in mesoscale applications (i.e. $\sim$10 hPa), the median absolute error with respect to a full atmospheric column is less than 0.5% in GHI, DHI and DIF and hence, ϵ_{tom} can be neglected.

  Among the schemes, the magnitude of this error is related to the approximation used for the layer between the TOM and the top of the atmosphere (TOA). Dudhia and FLG are the schemes more sensitive to variations in the TOM position because both parameterizations assume a transparent layer. The sensitivity is higher in FLG than in Dudhia because the first one includes the stratospheric ozone (neglected as the TOM is set at lower heights), while the second one only considers the contribution of the dry air.

  Goddard, New Goddard and RRTMG are the least dependent schemes because they assume an averaged ozone value for the layer between the TOM and the TOA.

  Finally, CAM is an intermediate case. This scheme assumes a constant ozone mixing ratio based on the value at the TOM. Consequently, when the TOM is located below the ozone layer, this scheme produces a high ϵ_{tom}. In contrast, the error decreases quickly when the TOM is set around the ozone layer.

- **Truncation error** (Fig. 7.2): The sensitivity of the solar schemes on the vertical configuration (i.e. number of levels and their distribution through the atmosphere) is directly related to the method used for the vertical integration of the multiscattering processes. Goddard, New Goddard, CAM and RRTMG are the schemes with the lower dependence on the verticals settings, while Dudhia and FLG show important variations, overall, when the number of vertical levels is less than 100.

  The first set of schemes use the adding method for the vertical integration of the multiscattering processes. This means that fluxes are evaluated in two stages: a first sweep from the TOA to the surface and a second sweep from the surface to the TOA. As a consequence, the errors due to the assumption of homogeneous atmospheric layers are compensated leading to more stable outcomes.

  In contrast, Dudhia and FLG present a single downward integration of the fluxes in which the errors are more evident. In the case of the FLG, this limitation may be corrected by including the adding method proposed by Zhang et al. (2013) for the δ-4-stream approximation.

  For the typical modeling configurations under clear-sky conditions, the median absolute error[1] of the GHI, DHI and DIF is around 1.1%, 0.9% and 4.9%, respectively with the RRTMG scheme achieving the lowest truncation error and the FLG and Dudhia parameterizations producing the highest error.

  It increases in both low and high cloud scenarios because cloud characteristics are very sensitive on the vertical settings. In the low cloud case, the median absolute error[2] is around 2.6% with respect the baseline case for the GHI and DIF. By schemes, CAM and RRTMG show the best skills while Dudhia and New Goddard the worst ones. In the case

[1] Considering the median of the absolute values presented in Tables 5.3 and 5.4 for a configuration of 80 vertical levels logarithmically distributed.

[2] Considering the median of the absolute values presented in Tables 5.5 for a configuration of 80 vertical levels logarithmically distributed.

of the DHI, the error can not be analyzed because all the schemes produce 0 values due to the high opacity.

In the high cloud case, the discussion becomes more complex. In a configuration based on a higher vertical resolution near to the surface than in the upper levels, the high cloud proposed is not well represented increasing the ϵ_{trunc} to 4.5% for GHI, 20.6% for DHI and 75.4% for DIF[3].

Figure 7.2: Infograph summarizing the main conclusions regarding the TOM and truncation errors. Values in gray indicate the median absolute error derived from the tables presented in Sect. 5.2. In the case of the truncation error, values are referred to a configuration with 80 vertical levels logarithmically distributed.

- **Physical error under clear-sky conditions** (Fig. 7.3): The study of the ϵ_{phys} at 6 stations of the BSRN distributed around the world reveals the same patterns for all the schemes. With the exception of Dudhia, the behavior is generally the same. A large

[3]Considering the median of the absolute values presented in Tables 5.6 for a configuration of 80 vertical levels logarithmically distributed.

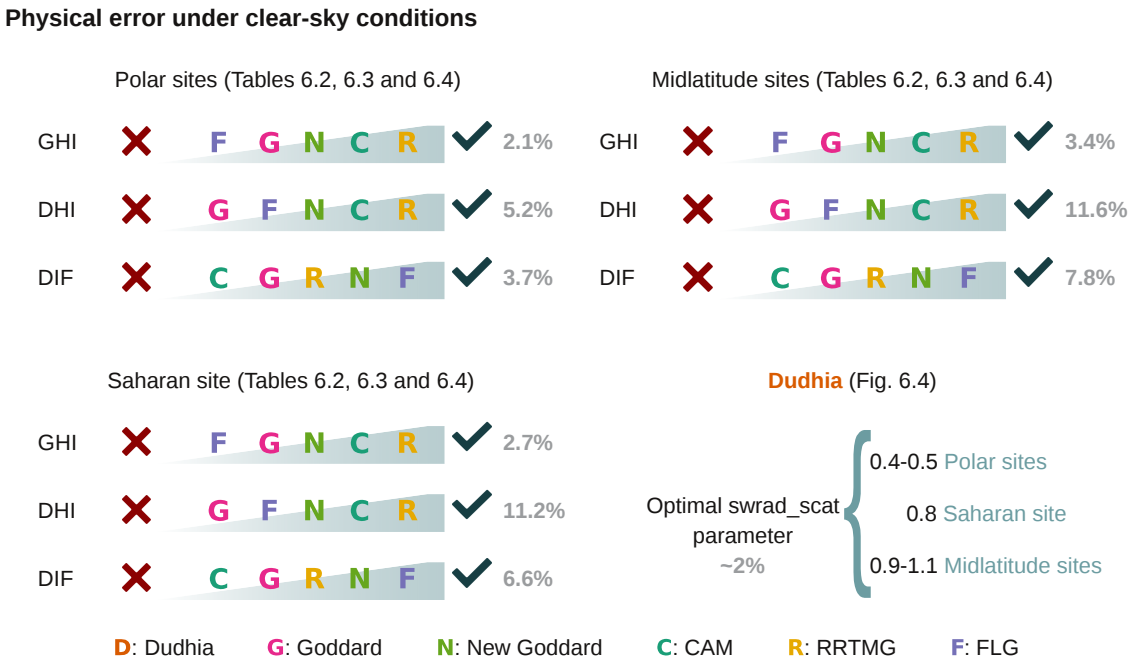

Figure 7.3: Infograph summarizing the main conclusions regarding the physical error. Values in gray indicates the mean absolute error derived from the tables presented in Sect. 6.2. The red cross indicates worse skills while the black check-mark means better skills.

overestimation of the DHI with a large underestimation of the DIF which leads to a near-zero bias for the GHI. The errors observed in the DHI and DIF accentuate the need for a global representation of the aerosols as many authors have been focused during the last years.

The RRTMG shows the most accurate results for GHI and DHI estimations, followed by CAM and New Goddard, while the worst results are obtained in Goddard and FLG. In contrast, the accuracy of the schemes in the determination of the DIF component is significantly different. FLG, New Goddard and RRTMG show the best performance while Goddard and CAM provide the less accurate results.

Based on the set of experiments presented in this thesis, sites located in polar regions experience the lowest errors with a mean nMAE of 2.1%, 5.2% and 3.7% for GHI, DHI and DIF, respectively, as a result of the low content of water vapor and aerosols.

By contrast, the midlatitude sites show the worst results with a mean nMAE of 3.4% in the GHI, 11.6% in the DHI and 7.8% in the DIF, as a consequence of a higher amount of water vapor and a more complex interaction with the aerosols.

As Dudhia can be calibrated by the swrad_scat parameter, this variable was optimized showing an asympotic nMAE around the 2% in all the sites. The optimal value in the polar sites is found between 0.4 and 0.5, in the Saharan site around 0.8 and in the midlatitudes sites ranging from 0.9 to 1.1.

Final remarks and future

After concluding this thesis, an obvious question arises: which is the most suitable parameterization for the solar resource modeling? The results and conclusions presented in the previous chapters show that RRTMG is the parameterization with the best skills. First, this scheme solves the RTE explicitly, leading to a full solution of the fluxes (i.e. direct and diffuse) necessary for photovoltaic and CSP applications. Second, this scheme is prepared for working with the radiative variables of the aerosols provided externally by the NWP model. This opens the door for a large number of developments such as coupling a chemical model (e.g. WRF-Chem) or with similar approaches that the ones proposed in Ruiz-Arias et al. (2012) and Ruiz-Arias et al. (2014), more feasible now. Moreover, this scheme shows a high stability with respect to the vertical configuration minimizing the ϵ_{tom} and ϵ_{trun}. Finally, the evaluation of the ϵ_{phys} under clear-sky conditions indicates that it is the most accurate parameterization in all the analyzed regions.

In spite of the initial determination of presenting a full analysis of the solar parameterizations, not all the elements have been studied in this thesis: the effect of the aerosols in the three components of the error, the ϵ_{phys} under cloudy situations and the uncertainty derived from the other components of the model. The analysis of these factors requires a different approach than the one presented in the previous chapters and hence, they have been shifted as a future work.

At this point, what is the future of the solar modeling? Solar resource modeling and more particularly the application of the WRF-ARW model has been improved significantly since this thesis started in 2011. The WRF-Solar project has been an essential starting point for this purpose. Nevertheless, new efforts will be necessary in the future in order to improve the aerosols representation within NWP models as well as to decrease the uncertainty associated with the cloud location and characteristics.

Ending, at the moment of writing this thesis, a new age in the atmospheric modeling is starting. The increment of the grid resolution is allowing to reach the microscale with resolutions of hundreds of meters (Montornès et al., 2016a,b), and even of tens of meters in the next years. In this context, the need of an accurate evaluation of the surface fluxes is increasing as one of the challenges for the mesoscale-microscale coupling. At these scales, grid-points are not longer independent and hence, the assumption of 1-dimensional independent columns (valid for synoptic and mesoscale applications) will need to be reformulated by using a 3-dimensional approaches including the interaction between the atmospheric columns. In this way, the studies presented in Wissmeier et al. (2013) and Jakub and Mayer (2016) establish the basis for this future development. Concurrently, the high amount of computational resources needed by the radiative transfer parameterizations will be improved by the incorporation of the computation based in GPUs and algorithms based on CUDA in the field of the atmospheric modeling (Lu et al., 2012; Price et al., 2014). All of this opens new horizons and challenges in the atmospheric modeling.